Modelling the Interaction of haemodynamics and the Artery Wall: Current Status and Future Prospects.

Lawford PV[1], Ventikos Y[4], Khir A[3], Atherton M[3], Evans D[1], Hose DR[1], Care CM[5], Watton PN[4], Halliday I[5], Walker DC[2], Hollis AP[5], Collins MW[3].

[1]Academic Unit Medical Physics and Clinical Engineering, University of Sheffield, UK.[2]Department of Computer Science, University of Sheffield, UK.[3]School of Engineering and Design, Brunel University, W. London, UK.[4] Institute of Biomedical Engineering, Department of Engineering Science, University of Oxford, Oxford, UK .[5]Materials Modelling Group, Materials and Engineering Research Institute. Sheffield Hallam University, Sheffield, UK.

Address for correspondence: Dr PV Lawford, Academic Unit of Medical Physics, Floor I, Royal Hallamshire Hospital, Glossop Road Sheffield, S10 2JF. Tel +44 (0) 114 2712078. p.lawford@sheffield.ac.uk

Summary

The arterial wall is exposed to mechanical forces associated with the flowing blood. *In vivo* the artery is subject to an axial load, a wall stress in the circumferential direction due to the internal pulsatile pressure and a frictional stress, the wall shear stress, generated by the moving blood. The cells are sensitive to changes in the magnitude and frequency of these stresses which are important modulators of cell function.

Deviation of the mechanical environment of the cells from homeostatic levels stimulates vessel wall remodeling, increasing the production of structural proteins and degradative enzymes until a new homeostatic state is achieved. The haemodynamic environment can give rise to deleterious remodeling, for example, atherosclerosis or aneurysms.

Clinical research has historically focused on the two main strategies of *in vivo* and *in vitro* experimentation. The concept of applying scientific theory to direct clinical applications is relatively recent. In this paper we focus on the interaction of wall shear stress with the endothelium and discuss how 'state of the art' computer modeling techniques can provide valuable data to aid understanding. Such data may be used to inform experiment and further, may help identify the key features of this complex system.

Key words: haemodynamics, endothelium, shear stress, atherosclerosis.

Introduction

The structure of the arterial wall (Figure 1a) is maintained by cells (endothelial cells, smooth muscle cells and fibroblasts) that degrade and deposit the structural proteins of which it is comprised. The functionality of these cells is regulated by mechanical signals associated with the pulsatile flow of blood through the lumen.

Figure 1 and Figure 2 here.

There are two types of stress on the vessel wall, one associated with mechanical equilibrium under the internal pressure and one associated with the viscous resistance of flowing blood (Figure 2). In vivo, the artery is a pre-stretched material under an internal pressure load (1). Internal pressure produces a stress in the circumferential direction. Neglecting viscoelastic and inertial effects in the vessel wall, circumferential stress is proportional to the instantaneous applied pressure. Interestingly, in addition to the cyclic circumferential stress an axial load is present. For unfixed human cerebral vessels the average *in vivo* axial stretch of is 1.31 (2). This mechanical environment results in typical circumferential stresses of 150KPa and typical axial stresses of 75 to 125KPa (3).

The flow is driven by a pressure gradient along the axis of the vessel. It is often assumed that the velocity of the blood at the wall of the vessel is zero (the no-slip boundary condition), and the frictional stress generated at the wall by the moving blood sliding over this stationary layer is called the wall shear stress (WSS). The cells are sensitive to changes in the magnitude and frequency of these stresses and both are important modulators of cell function. The internal pressure, and thus the circumferential stress, typically varies rapidly in time but only slowly in space. The cyclic stress, or the change in stress over the cardiac cycle, might be as important as the absolute magnitude of stress. As the pressure gradient changes over the cardiac cycle, so too the WSS changes. The oscillatory shear index (OSI) is a measure of the change of direction of the flow over the cardiac cycle. In the smaller vessels the flow is essentially unidirectional thus the OSI is zero. In larger arteries there is often some reverse flow at some point in the cardiac cycle, giving rise to oscillatory shear stresses. Significant oscillatory shear is, however, usually found only in regions of geometrical irregularity causing flow separations and local vortex structures.

Deviation of the mechanical environment of the cells from homeostatic levels stimulates vessel wall remodeling, increasing the production of structural proteins and degradative enzymes until a new homeostatic state is achieved. The haemodynamic environment can give rise to deleterious remodeling. For example, atherosclerotic lesions are found preferentially at bifurcations (4) and

the development of cerebral aneurysms is thought to be intimately linked to the WSS (5-8) although the exact mechanisms remain unknown.

In this paper we focus on the interaction of WSS with the endothelium and discuss how 'state of the art' computer modeling techniques can provide valuable data to aid understanding. Such data may be used to inform experiment and further, may help identify the key features of this complex system.

The endothelium forms a permeability barrier between blood flow and the underlying tissues of the vessel wall and regulates aspects of circulatory function. A "healthy" endothelium favours vasodilatation, provides an anticoagulant, profibrinolytic boundary, thus inhibiting leukocyte adhesion and platelet aggregation, and exhibits anti-inflammatory, anti-proliferative and anti-oxidant characteristics conducive to the maintenance of a functional artery. Given this strategic role, it is not surprising that a dysfunctional endothelium, characterised by a reduced bioavailability of vasodilators and heightened state of endothelial activation, functions as a key mediator in the pathogenesis of arterial disease (9,10).

The physical properties, structural arrangement and morphology of endothelial cells (ECs) are influenced by local mechanical forces. Shear stress increases the stiffness and alters the viscous properties of these cells (11). *In vitro*, ECs elongate, changing from a polygonal 'cobblestone' morphology to flattened, elongated ovoids under the influence of flow (Figure 1b). The degree of elongation correlates with the magnitude of the shear stress (12-15). The type of shear stress is also relevant as, under oscillatory shear, cultured cells retain a polygonal shape (13). *In vivo,* cells have been shown to orientate with the predominant local flow direction (16) and perpendicular to the direction of cyclic stretch (17) but the relative importance of the two different mechanical stimuli for the normal *in vivo* state is not clear (18). Furthermore, local topography may itself influence local shear stress; alignment of ECs with the direction of flow reduces the maximum shear stress by 50% (12) demonstrating the intimate coupling between shear stress and endothelial organisation and morphology.

In normal arteries, the magnitude of WSS typically ranges between 10 and 70 dynes/cm^2 (1-7 Pa). A mean positive steady shear stress is thought to be the optimal situation and is characterised by low proliferation and increased cell survival times. A number of beneficial effects are reported; cells align with the flow; integrin distribution is reorganized improving endothelial cell adhesion and anti-thrombic and vasoactive agents, namely nitric oxide, endothelium-derived hyperpolarizing factor, prostacyclin and endothelin are produced (19,20). These act on the adjacent vascular smooth muscle cells which regulate the diameter of the

vessel and thus control the local blood flow rate (21). Locally-mediated regulation of vessel diameter helps to maintain WSS within the normal range.

As discussed above, higher and lower values of WSS and of OSI are found at specific sites in the circulation in association with changes in geometry (a curvature, bifurcation, anastomosis or stenosis, for example) with the lowest values being found where the flow becomes unstable with associated flow separation, recirculation zones or stagnant regions. Specific levels of shear stress are believed to result in increased levels of biomarkers associated with inflammatory pathways and ultimately predispose to atherosclerosis. Historically, high WSS is considered atheroprotective (22), whereas low WSS is associated with atherogenesis (10). A number or studies suggest that oscillatory shear is also detrimental; for example, Ku *et al* (23), report a correlation between atherosclerotic plaque location and areas of low and oscillating WSS in the human carotid bifurcation. An additional level of complexity is demonstrated by the results of *in vitro* studies indicating that ECs can sense temporal and spatial gradients of WSS (24-26).

A membrane-bound macromolecular coating on the luminal surface of the endothelial cell, the glycocalyx, provides the interface between the endothelium cell and the blood. Comprising sulphated proteoglycans, hyaluronan and glycoproteins, the glycocalyx has a net negative charge and is enhanced by the binding of blood-born molecules such as plasma proteins, enzymes cytokines, water and other molecules with cationic sites forming a layer ~500nm thick (27). As well as having a key function with respect to permeability and leukocyte interactions, it is believed to act as the primary mechano-transducer of fluid shear stress to the cytoskeleton (28).

Mechano-transduction plays a key role in both the regulation of blood pressure and vessel response to shear stress. Shear stress is transduced into chemical signals which activate signalling pathways controlling cell functionality, *i.e.* gene and protein expression (17). Mechanical stimuli are also converted into intracellular signals that affect the proliferation, apoptosis, migration and permeability of the ECs and remodelling of the arterial wall (24,29).

Whilst there is a substantial literature describing the influence of shear stress on ECs, most data has been obtained from *in vitro* experiment using rigid flow chambers and well-characterised flows. In this situation, WSS can be calculated with a reasonable level of confidence. *In vivo,* the situation is more complex and WSS is estimated from the mean volumetric flow and velocity of blood recorded in the vessel, vessel diameter and blood viscosity. The values obtained represent the average value of WSS over a considerable area of the vessel wall and encompass populations of ECs rather than being descriptive of the level of exposure of the individual cell. It can be argued that this is a reasonable approximation as there is evidence to suggest that there is significant interaction and intercellular signaling between ECs (30). However it is not clear over

what length-scale this effect operates and the shear force experienced by an individual cell or small populations of cells of may be important.

As will be seen, computational models of varying complexity can be used to give insight into some of these issues.

Application of Computational Fluid Dynamics to Blood Flow

Parallel with the introduction of computers since the Second World War has been the development of numerical methods, which enabled the governing partial differential equations to be modelled by equivalent equations which could be solved computationally (for example, finite difference equations). These started to be of engineering significance in the 1960's for solid stress analysis, where the fundamental science was applied to discrete small areas, termed finite element analysis.

For fluids, the real breakthrough came at the end of the 1980's when the first commercial Computational Fluid Dynamics (CFD) codes were introduced. These enabled real problems to be addressed. The codes were rapidly developed to be able to investigate three-dimensional (even time-dependent) irregular geometries. Using the first release of the CFD code FLOW3D one of us (MWC) initiated research into the haemodynamics of arterial bifurcations. A review by Xu and Collins (31) showed that, in order to be meaningful clinically, a model should have the potential to address: a] the time-dependent pulsatility of blood flow, b] the non-Newtonian character of blood (ie the non-linear relationship between viscosity and shear stress), c] the 3D geometry of the arterial system, and d] its time-dependence due to the distensibility of the arterial wall.

A number of data sources are essential to the development of a computational model. For cardiovascular models these include; a description of the boundary conditions (the set of conditions specified for the behaviour at the boundary of the domain), a 3D description of the geometry, a description of the material behaviour (eg. blood viscosity and arterial stiffness) and the availability of an appropriate set of validation data against which some basic feature of the output of the model can be tested. Boundary conditions are important in determining the mathematical solutions to many physical problems and compensate for the fact that it is not feasible to model a system in its entirety. In the context of a cardiovascular model they include physical properties such as pressure or flow at the inlet and outlet of the domain. An *in vitro* set of experiments by carried out by Moravec and Liepsch (32) involved these four aspects, and was used as a test for the model (33), as were subsequent *in vivo* canine bifurcation data (34). The model was then extended to be able to use clinical Magnetic Resonance (MR) data for input boundary conditions for the CFD code; this also involved image processing studies (35). Finally,

the addressing of wall distensibility (a fluid-structure interaction-FSI-problem) proved a challenging task. Because of the complexity and non-linearity of the Navier-Stokes equations, only a few analytical solutions exist, and it is noteworthy that one of these 'classic' fluid dynamic cases, that of Womersley (36), related to pulsatile blood flow and arterial wall movement. A number of alternative FSI models were successfully tested by the group in question, all using Womersley's data for code validation (37).

CFD codes have now been combined with solid mechanics FEA codes to give immediate FSI capability. One barrier to using this approach for cardiovascular vessels is the lack of information on the constraints applied to vessel wall motion *in vivo*. An alternative solution is to use time series image data to prescribe wall motion. The Sheffield group recently used this method in a study characterising the haemodynamics of the human superior mesenteric artery (SMA). This work was motivated by the observation that, in comparison to many other arteries, the SMA is largely spared from primary atherosclerotic disease (38). The parent vessel, the abdominal aorta, has been shown to be a principal site for the development of atherosclerotic lesions (39) as are the immediate proximal (coeliac) and distal (renal) branches. A fully transient, CFD model was constructed of a segment of the abdominal aorta and SMA. The geometry was based on dynamic MR imaging data and boundary conditions (flow), were determined from phase contrast MR velocity measurements (40).

Figure 3

The resulting OSI map for the model is shown in Figure 4a. OSI is, in general, lower in the SMA than in the aorta. The only area of high OSI in the SMA is at the root of the vessel as it leaves the aorta. This and correlates with clinical observations for atheroma. Figure 4b illustrates the time varying WSS for two areas of the vessel wall exposed to a high or low level of OSI.

The sequence described above exemplifies how basic science expressed in novel technology can be incorporated into clinical research and early demonstrators of the integration of a simulation chain into a clinical workflow are taking place in the AneurIST project (www.aneurIST.org).

Introducing an additional level of complexity, some of the concepts discussed previously (computational assessment of haemodynamic loads, tissue remodelling, endothelium signaling etc.) can be incorporated in coupled computational simulation frameworks that enable us to examine the interaction of the various physiological processes and evaluate the relative importance of mechanisms that are explicitly incorporated into such models. The models have practical applications, in particular, for disease evolution prediction for patient-specific cases.

Moreover, they are proving invaluable in the challenging task of hypothesis evaluation; they are highly effective tools to test and evaluate competing theories, since they allow the interrogation of disease progress scenarios.

Simulation of the evolution (inception, growth and rupture) of cerebral aneurysms by the group at the University of Oxford provides an illustrative example of this type. Aneurysm risk evaluation involves a variety of factors including; genetics, geometry of the vasculature, mechanical properties of the tissue and blood flow details and is therefore a particularly sensitive and biologically-dependent process.

The first stage is to estimate the haemodynamic loads (pressure and WSS) that act on the aneurysm (and parent artery) using a finite volume technique. The distribution of WSS on the inner surface of the aneurysm is computed and used to model the hypothetical response of the endothelium, which subsequently signals the smooth muscle cells and fibroblasts and leads to a remodeling and growth/atrophy of the elastin and collagen in the arterial wall. This results in changes in the mechanical properties of the aneurysm and the geometry adapts to maintain mechanical equilibrium; a finite element method is used to solve the updated deformation field. The new geometry will result in a change in the haemodynamics and thus the WSS distribution. The updated flow field is solved and the computational cycle is repeated until the aneurysm stabilises in size or until the loads imposed exceed the load-bearing capacity of the wall leading to rupture.

Figure 4

Such integrative models can be used to evaluate whether hypothesised growth mechanisms yield predictions consistent with *in vivo* and *in vitro* observations, eg. relating the growth and remodeling of the arterial wall to the haemodynamic stimuli that act on the ECs. For instance, the magnitude of the spatial WSS gradient (WSSG) has been proposed as one possible haemodynamic parameter which is correlated with regions of pathological remodelling (7,41). As an aneurysm adapts the WSSG spatial distribution (see Figure 4) acting on the endothelium will change substantially and thus an understanding of how this affects the subsequent remodeling of the tissue is of critical importance. Current research focuses on investigating hypotheses coupling the remodeling to such haemodynamic influences.

Requirement for Analyses on Micro and Mesoscales.

Now that macro-scale modelling is relatively commonplace, current focuses include the necessity to investigate very fine scales together with their impact on behaviour at conventional scales and at the levels of the organ and organism. Work in progress at the University of Brunel

investigating the interaction of intravascular devices with the arterial wall, specifically; the Intra Aortic Balloon Pump (IABP) and vascular stent demonstrates a need to address smaller scales in general and the endothelium (and possibly the glycocalyx) in particular.

The Intra Aortic Balloon Pump (IABP) is a widely-used cardiac assist device. The balloon, usually inserted in the abdominal aorta via the iliac artery, is inflated and deflated every-, every other- or every second cardiac cycle. Inflation takes place during diastole and deflation during systole with the aim of increasing coronary flow and reducing left ventricular after-load. Inevitably, the balloon contacts the inner wall of the aorta with every inflation/deflation cycle. This repeated event (and possible contact with atherosclerotic plaque) has been reported to be responsible for balloon rupture. However, no systematic study has been performed to investigate the mechanical effects of balloon/wall interaction. Furthermore, as the balloon approaches the endothelium, a volume of blood is displaced proximally and distally. This squeezing process generates shear stresses which, as yet, remain to be quantified. Similarly, when the balloon moves away from the endothelium during deflation, it will generate micro pressure differences that may impose stretching (pulling) stresses on the ECs. A very high spatial resolution is required in order to understand this process fully and to interpret the effects at the cellular level.

As this issue has not been investigated, manufacturers have made no attempt to increase the diameter of the balloon, despite their conviction that a larger diameter would yield a better clinical outcome. Improved understanding of the balloon/wall interaction may allow the balloon diameter to be increased whilst reducing the risk of adverse events. If the balloon is inflated and deflated once every cardiac beat, for an average patient using the IABP for 3 days, there will be approximately 250,000 incidents of frictional contact between balloon and aortic wall. Data is available on the effect of imposing stresses on the endothelium layer for a few hours (42) but the influence of cyclical effects for longer periods is unknown. The answer to this question may offer clinicians a maximum safe period for using the IABP before the endothelium begins to be damaged.

Information on micro-scales is also important when evaluating the performance of vascular stents. Stenting has two primary clinical objectives: to mechanically dilate a stenosed artery and to have minimal detrimental impact upon local blood flow characteristics. Stents are clearly effective in opening up diseased arteries and restoring flow. However, at the near-wall micro-scale, the situation is less satisfactory. The thin (~100μm) stent struts apply stresses to the endothelium and glycocalyx and the local flow is disturbed causing further interaction with endothelial topography. Macroscopic models, such as those described by Raedelli et al capture important details of the flow but are not resolved to cellular and sub-cellular length-scales (43)

Recent numerical modelling studies investigated the effect of endothelial topography on the calculation of WSS (44),(45). The influence of pulsatile flow on WSS is also of interest in terms of the temporal values that exceed certain high or low values, often associated with recirculation near the stent wires especially on the leeward side(46). In describing performance, a key challenge is how to summarise the spatial and temporal WSS values, without loss of important information.

Considerable computing resource is required to model a stented artery in its entirety with resolution of the fine detail of the stent struts and local blood flow. So much so, that often studies are confined to a 'representative' portion of the stented artery. This assumes symmetry, which is frequently not the case, and means that understanding the role of the stent as a whole is obscured. Add to this an interest in the interaction of the stent with blood cells, ECs and/or the glycocalyx and the model resolution required becomes too demanding for resolution with sufficient detail with conventional CFD. As will be discussed below, one way of a addressing this is to use a multi-scale approach.

Multi-scale and multi-physics modelling techniques.

There is ever-increasing accessibility of relatively inexpensive computing power but the tendency is to create models of increasing complexity thus challenging whatever computational resource might be available. The optimal strategy is *to use models of no greater detail than the processes for the particular scale demand.* Multi-scale modeling embodies the efficient combination of such scale-related models and it is increasingly used in science and engineering as a powerful tool for making simulation of complex biological systems computationally tractable. This approach has been adopted in the successful UPS *Physiome Project* (47).

Human physiology systems are multi-scale, multi-science systems, encompassing a range of phenomena including molecular and cellular biology, physics, medicine, and engineering and crossing many orders of magnitude in terms of temporal and spatial scales. The challenge is how best to integrate these different aspects into the model. An approach is needed to break the system down into a number of single-scale models which can then be coupled and interact across the scales.

A Scale Separation Map (SSM) on which each single-scale system is represented as an area according to its spatial and temporal scales helps in the identification of key processes having well-separated scales as the components of the multi-scale model. The EU-funded COAST [Complex Automata Simulation Technique] project (www.complex-automata.org)(48) is developing this concept and employing it to model the complex process of coronary artery in

stent restenosis. Details can be found in Evans *et al* (49). To illustrate the principles of this modeling paradigm a SSM has been developed demonstrating how the interaction of blood flow and the vessel wall can be represented in this way.

Figure 5 here.

It must be emphasised that the SSM is not a definitive representation of a system. The placement and degree of resolution of sub-systems reflects the extent of the domain which is to be modelled and the availability of quantitative data to support the models. The map aims only to provide information about how any two processes are separated and must subsequently be coupled. An interesting observation is that the biologists, clinicians, physicists and engineers working on the development of the SSM found it to be a very useful conceptual tool for arranging, cataloguing and formalising existing knowledge, and for identifying gaps in the current knowledge base and thus informing future experiments.

Within the COAST project agent-based models are used to represent the ECs and smooth muscle cells. The software agent is an intuitively natural computational representation of a real world entity. It is applicable to any system where emergent behaviour arises as a result of the complex interactions between many individuals, and is particularly appropriate in the case of modeling biological tissues where tissue behaviour is an emergent property of the responses and interactions of individual cells. At the simplest level, the observed behaviour of the real-world cells are represented by simple logical rule sets that determine the responses of individual software agents to various stimuli (eg rules can represent apoptosis, change in morphology or progression through the cell cycle in response to a sensed diffusive signal or a shear stress). This paradigm has previously been used to model the behaviour of growing epithelial cell populations, and the response of confluent monolayers to scratch wounding (50,51). The application of agent modeling of endothelial tissue allows the potential heterogeneity of individual ECs to be explicitly represented, with each cell permitted to react differently depending on its gene/protein expression and differences in the local modeled flow field. Sub-models of signaling processes could also be incorporated as an extension to the logical rule sets, thus adding a further layer of complexity to the model.

Another possibility is to explicitly include the blood cells in the flow model. The CFD analyses described previously treat blood as a continuous fluid flow and represent the vascular endothelium as a constant, locally smooth velocity (Dirichlet) boundary condition. In reality, the vessel walls encounter Newtonian plasma, which advects discrete, embedded cells. These will encounter the vessel wall in different ways, according to local flow conditions, geometry and cell concentration.

10

Figure 6

Figure 6, represents a simplified, two-dimensional calculation of flow in the region of an explicitly modelled single detaching leukocyte, traditionally represented as a wetting drop of immiscible fluid. These results, obtained using multi-component lattice Boltzmann (LB) simulation, illustrate the complexity of flow in the region of a single cell contact with an idealised boundary. Plainly there is no such thing as a microscopically steady WSS - even in steady macroscopic vessel flow. Little imagination is necessary to see that, at normal haematocrit concentrations of advected erythrocytes, near-wall flow (and hence WSS distribution) becomes exceedingly complex. Retaining such short length and time scale physics is central to understanding the response of ECs. To do so requires novel flow computation methods which are "two-way coupled" to the agent models (as outlined above) and which can also address other issues discussed briefly below. Capture of complex interactions between a representative number of explicitly modelled erythrocytes is necessary and the need to model ingress of atherosclerotic agents at exposed endothelial cell boundaries (to inform coupled agent models) requires coupled plasma species diffusion-advection. Therefore, a multi-physics flow technique, able efficiently to handle many erythrocytes, is required. Incorporation of the cellular WSS morphological response (mediated by agent models) as explicitly resolved, geometrically complex Dirichlet boundary conditions requires a suitably adaptable flow technique. Finally, the overall computational demands point to a parallelizable algorithm. The multi-component LB Equation simulation method has all these attributes (52). The application of this particular variant of LB used to obtain the data shown in figure 6 (53) to the problem of wetting is described in detail in Hollis et al (54).

CONCLUSIONS

The use of computational methods for medical applications is now commonplace in the research community but not, as yet, in routine clinical practice. Complex simulation chains which facilitate CFD analyses of models developed from patient-specific geometries are capable of providing information which, because of limitations of current investigative techniques (in terms of resolution or the need for direct visualisation by microscopic imaging of fluorescent particles for example), is not available from clinical studies or experiment (Reneman et al 2006).

The ultimate aim is to produce systems which couple haemodynamics with models of biological phenomena to test hypotheses or predict the likely outcome of a disease or an intervention; the potential power of such models is beginning to be recognised and new technologies are being developed in order to cope with the challenges presented by such complex systems. This includes methodology to enable the integration of models of different type, levels of complexity and scales. However, the greatest challenge, and the ultimate goal, is the translation of this

11

technology to the clinical arena. Data reduction is a key element; models can produce complex and detailed outputs which must be summarised to give clinical meaningful indices. It must also be borne in mind that the engineering procedures of code validation/verification need to be carefully followed. Access to validation data is of paramount importance and it is essential clinicians and biologists are engaged fully at an early stage. The final tools must also be tested and validated by the clinical end users.

A number of exciting initiatives are poised to accelerate progress and uptake in this area. In recognising the potential of ICT-based tools for modeling and simulation of human physiology and disease-related processes, the EU is funding a number of collaborative projects directed towards the development of patient-specific computer models for personalised and predictive healthcare under the banner of the *Virtual Physiological Human(55)* (56). A networking action (the VPH Network of Excellence) within the recent funding call will support the research community, and lay foundations for methodological, technical and training frameworks to support such research.

The authors wish to acknowledge the support of the EU Sixth Framework programme (AneurIST, COAST) and BRET (The Bardhan Research and Education Trust) for aspects of this work.

References

1. Holzapfel, G. A., Gasser, T. C., and Ogden, R. W. (2000) *Journal of Elasticity* **61**(1-3), 1-48

2. Monson, K. L., Goldsmith, W., Barbaro, N. M., and Manley, G. T. (2003) *J Biomech Eng* **125**(2), 288-294

3. Gleason, R. L., Taber, L. A., and Humphrey, J. D. (2004) *Journal of Biomechanical Engineering-Transactions of the Asme* **126**(3), 371-381

4. De Keulenaer, G. W., Chappell, D. C., Ishizaka, N., Nerem, R. M., Alexander, R. W., and Griendling, K. K. (1998) *Circ Res* **82**(10), 1094-1101

5. Ahn, S., Shin, D., Tateshima, S., Tanishita, K., Vinuela, F., and Sinha, S. (2007) *J Magn Reson Imaging* **25**(6), 1120-1130

6. Burleson, A. C., Strother, C. M., and Turitto, V. T. (1995) *Neurosurgery* **37**(4), 774-782; discussion 782-774

7. Meng, H., Wang, Z., Hoi, Y., Gao, L., Metaxa, E., Swartz, D. D., and Kolega, J. (2007) *Stroke* **38**(6), 1924-1931

8. Shojima, M., Oshima, M., Takagi, K., Torii, R., Hayakawa, M., Katada, K., Morita, A., and Kirino, T. (2004) *Stroke* **35**(11), 2500-2505

12

9. Bonetti, P. O., Lerman, L. O., and Lerman, A. (2003) *Arterioscler Thromb Vasc Biol* **23**(2), 168-175

10. Caro, C. G., Fitz-Gerald, J. M., and Schroter, R. C. (1971) *Proc R Soc Lond B Biol Sci* **177**(46), 109-159

11. Sato, M., Ohshima, N., and Nerem, R. M. (1996) *J Biomech* **29**(4), 461-467

12. Barbee, K. A., Davies, P. F., and Lal, R. (1994) *Circ Res* **74**(1), 163-171

13. Helmlinger, G., Geiger, R. V., Schreck, S., and Nerem, R. M. (1991) *J Biomech Eng* **113**(2), 123-131

14. Levesque, M. J., Liepsch, D., Moravec, S., and Nerem, R. M. (1986) *Arteriosclerosis* **6**(2), 220-229

15. Levesque, M. J., and Nerem, R. M. (1985) *J Biomech Eng* **107**(4), 341-347

16. Malek, A. M., Alper, S. L., and Izumo, S. (1999) *Journal of the American Medical Association* **282**(21), 2035-2042

17. Chien, S. (2007) *Am J Physiol Heart Circ Physiol* **292**(3), H1209-1224

18. Owatverot, T. B., Oswald, S. J., Chen, Y., Wille, J. J., and Yin, F. C. (2005) *J Biomech Eng* **127**(3), 374-382

19. Korenaga, R., Ando, J., Tsuboi, H., Yang, W., Sakuma, I., Toyo-oka, T., and Kamiya, A. (1994) *Biochem Biophys Res Commun* **198**(1), 213-219

20. Malek, A., and Izumo, S. (1992) *Am J Physiol* **263**(2 Pt 1), C389-396

21. Levick, J. R. (2003) *An introduction to cardiovascular physiology*, Arnold, London

22. Carlier, S. G., van Damme, L. C. A., Blommerde, C. P., Wentzel, J. J., van Langehove, G., Verheye, S., Kockx, M. M., Knaapen, M. W. M., Cheng, C., Gijsen, F., Duncker, D. J., Stergiopulos, N., Slager, C. J., Serruys, P. W., and Krams, R. (2003) *Circulation* **107**(21), 2741-2746

23. Ku, D. N., Giddens, D. P., Zarins, C. K., and Glagov, S. (1985) *Arteriosclerosis* **5**(3), 293-302

24. LaMack, J. A., Himburg, H. A., Li, X. M., and Friedman, M. H. (2005) *Ann Biomed Eng* **33**(4), 457-464

25. Tardy, Y., Resnick, N., Nagel, T., Gimbrone, M. A., Jr., and Dewey, C. F., Jr. (1997) *Arterioscler Thromb Vasc Biol* **17**(11), 3102-3106

26. White, C. R., Haidekker, M., Bao, X., and Frangos, J. A. (2001) *Circulation* **103**(20), 2508-2513

27. Weinbaum, S., Tarbell, J. M., and Damiano, E. R. (2007) *Annu Rev Biomed Eng* **9**, 121-167

13

28. Pahakis, M. Y., Kosky, J. R., Dull, R. O., and Tarbell, J. M. (2007) *Biochem Biophys Res Commun* **355**(1), 228-233

29. Zhao, S., Xu, X., and Collins, M. (1998) *Proceedings of the Institution of Mechanical Engineers, Part H: Journal of Engineering in Medicine* **212**(4), 241-252

30. Demer, L. L., Wortham, C. M., Dirksen, E. R., and Sanderson, M. J. (1993) *Am J Physiol* **264**(6 Pt 2), H2094-2102

31. Xu, X. Y., and Collins, M. W. (1990) *Proc Inst Mech Eng [H]* **204**(4), 205-216

32. Moravec, S., and Liepsch, D. (1983) *Biorheology* **20**(6), 745-759

33. Collins, M. W., and Xu, X. Y. (1990) A predictive scheme for flow in arterial bifurcations: comparison with laboratory measurements. In: al., F. M. e. (ed). *Biomechanical Transport Processes* Plenum Press.

34. Xu, X. Y., Collins, M. W., and Jones, C. J. (1992) *J Biomech Eng* **114**(4), 504-511

35. Long, Q., Xu, X. Y., Collins, M. W., Griffith, T. M., and Bourne, M. (1998) *Crit Rev Biomed Eng* **26**(4), 227-274

36. Womersley, J. R. (1957) The mathematical analysis of the arterial circulation in a state of oscillatory motion. In., Wright Air Development Centre, USA

37. Xu, X. Y., Collins, M. W., and Jones, C. J. H. (1997) *Adv. Eng. Softw.* **28**(6), 365-377

38. Glagov, S., Zarins, C., Giddens, D. P., and Ku, D. N. (1988) *Arch Pathol Lab Med* **112**(10), 1018-1031

39. Roberts, J. C. J., Moses, C., and Wilkins, R. H. (1959) *Circulation* **20**(4), 511-519

40. Jeays, A. D., Lawford, P. V., Gillott, R., Spencer, P., Barber, D. C., Bardhan, K. D., and Hose, D. R. (2007) *J Biomech* **40**(9), 1916-1926

41. DePaola, N., Gimbrone, M. A., Jr., Davies, P. F., and Dewey, C. F., Jr. (1992) *Arterioscler Thromb* **12**(11), 1254-1257

42. Brooks, A. R., Lelkes, P. I., and Rubanyi, G. M. (2002) *Physiol Genomics* **9**(1), 27-41

43. Radaelli, A. G., Sola, T., Vivas, E., Mellado, X., Guimaraens, L., Cebral, J. R., and Frangi, A. F. (2007) Combined clinical and computational information in complex cerebral aneurysms: application to mirror cerebral aneurysms. In: Manduca, A., and Hu, X. P. (eds). *Proc. SPIE Medical Imaging 2007: Physiology, function, and structure from medical images.*

44. König, C. S., Long, Q., Collins, M. W., and Xu, S. (2006) *Biomedicine and Pharmacotherapy* **60**(8), 481

45. Davies, P. F., Zilberberg, J., and Helmke, B. P. (2003) *Circ Res* **92**(4), 359-370

14

46. Berry, J. L., Santamarina, A., Moore, J. E. J., Roychowdhury, S., and Routh, W. D. (2000) *Ann. Biomed. Eng.* **28**((4)), 386–398

47. Crampin, E. J., Halstead, M., Hunter, P., Nielsen, P., Noble, D., Smith, N., and Tawhai, M. (2004) *Exp Physiol* **89**(1), 1-26

48. Hoekstra, A., Lorenz, E., Falcone, J., and Chopard, B. (2007) *International Journal for Multiscale Computational Engineering* **5**, 491-502

49. Evans, D. J. W., Lawford, P. V., Gunn, J., Walker, D., Hose, D. R., Smallwood, R. H., Chopard, B., Krafczyk, M., Bernsdorf, J., and Hoekstra, A. G. (2008) *Philosophical Transactions of the Royal Society A* ***In Press***

50. Walker, D. C., Hill, G., Wood, S. M., Smallwood, R. H., and Southgate, J. (2004) *Ieee Transactions on Nanobioscience* **3**(3), 153-163

51. Walker, D. C., Southgate, J., Hill, G., Holcombe, M., Hose, D. R., Wood, S. M., Mac Neil, S., and Smallwood, R. H. (2004) *Biosystems* **76**(1-3), 89-100

52. Succi, S., Benzi, R., and Higuera, F. (1991) *Physica D* **47**(1-2), 219-230

53. Halliday, I., Hollis, A. P., and Care, C. M. (2007) *Physical Review E* **76**(2), -

54. Hollis, A., Halliday, I., and Care, C. M. (2006) *Journal of Physics a-Mathematical and General* **39**(33), 10589-10601

55. http://www.biomedtown.org/biomed_town/STEP/Reception/step-definitions/VirtualPhysiologicalHuman. (2007) Virtual Physiological Human. In.

56. Fenner, J. W., Brook, B., Clapworthy, G., Coverney, P., Feipel, V., Gregersen, H., Hose, D. R., Kohl, P., Lawford, P., McCormack, K. M., Pinney, D., Thomas, S. R., Van Sint Jan, S., Waters, S., and Viceconti, M. (2008) *Philosophical Transactions of the Royal Society A* ***In Press***

15

Figure Legends

Figure 1 Schematic model of the major components of a healthy elastic artery showing the three layers of the wall: the intima, media and adventitia and the distribution of endothelial and smooth muscle cells.

Figure 2 a The mechanical environment of the artery showing the distribution of stresses in the wall. **b.** The influence of shear stress on endothelial cell morphology.

Figure 3 Subject-specific CFD model of the abdominal aorta and a major branch, the superior mesenteric artery. Figure 3a shows distribution of OSI. The region of high OSI (arrowed) the proximal lip of the outlet of the origin of the SMA from the aorta corresponds with the normal distribution of atheroma reported for this artery. Figure 3b shows plots of different time varying WSS at two locations on the vessel wall. One corresponds to an area of high OSI (top) and the second to an area of low OSI (bottom).

Figure 4 Evolution of the wall shear stress spatial gradient [Pa/m] for an idealised aneurysm with a localized daughter bleb developing on the dome. Development of the aneurysm is accompanied by an increase in the WSSG around it's base: this may have significant implications for the degenerative remodelling of the tissue in this region and thus future growth of the aneurysm. At /t/=10, a daughter bleb begins to develop on the aneurysm dome. It can be seen that an annulus of high WSSG forms around the daughter bleb (/t/=12). This may result in further degeneration of the tissue in this region thus promoting the growth and enlargement (and possibly rupture) of the secondary bleb.

Figure 5 Scale Separation Map (SSM) The SSM is defined as a two dimensional map with the horizontal axis coding for temporal scales and the vertical axis for spatial scales. Each subsystem occupies a certain area on this map. Arrows indicate coupling between the single scale sub-systems.

Figure 6 A time sequence figure produced with a lattice Boltzmann simulation. It shows a 2D drop initially attached to a flat boundary, subject, at time t=0, to a shear. The dark / light background shading identifies immiscible fluid components, the overlying contours a rectangular stream function *calculated in the rest frame of the fluid*.

16

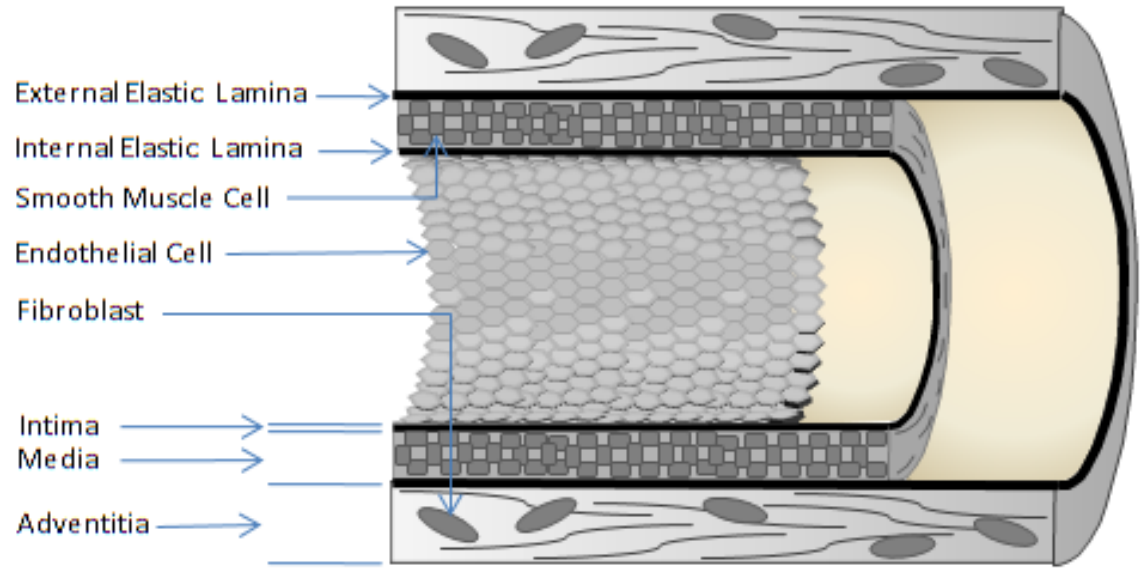

a)

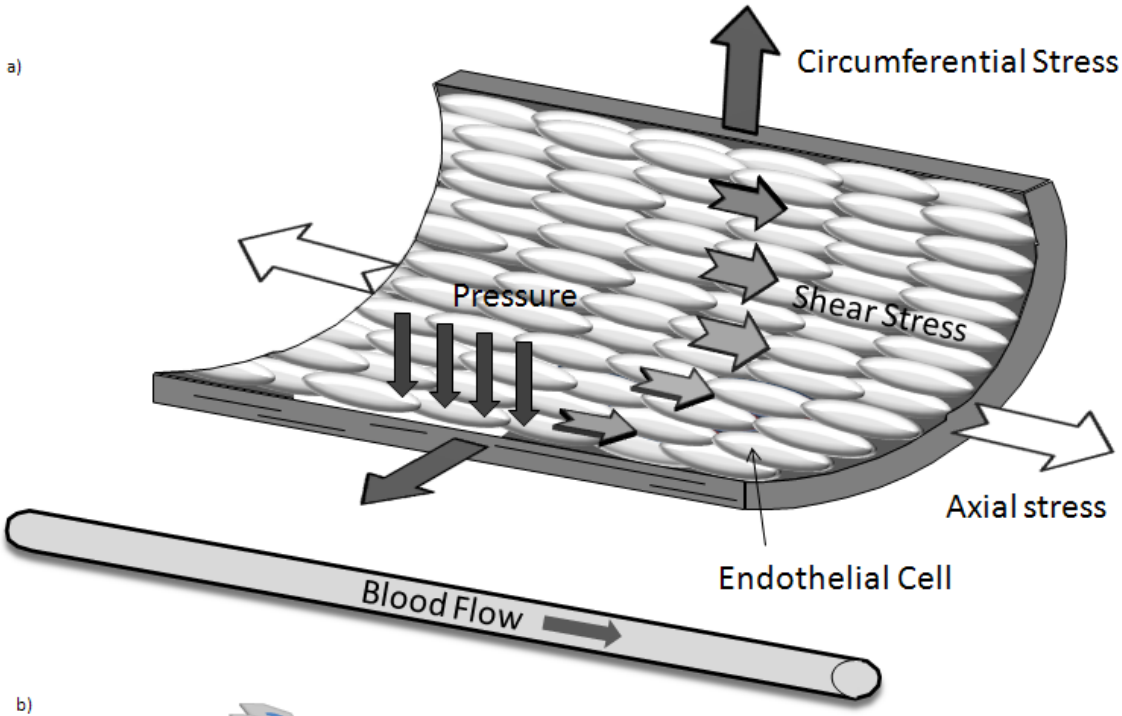

b)

"Healthy" Endothelium

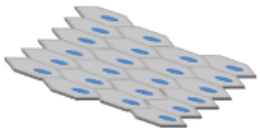

Endothelium exposed to Oscillatory or Low shear Stress

17

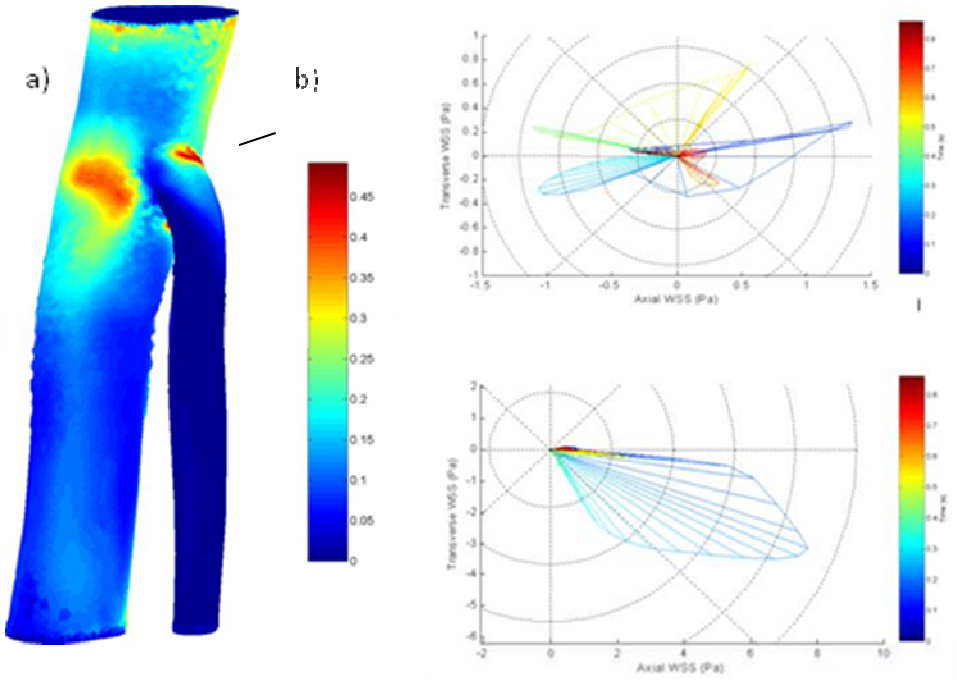
a)
b)
Transverse WSS (Pa)
Axial WSS (Pa)
Transverse WSS (Pa)
Axial WSS (Pa)

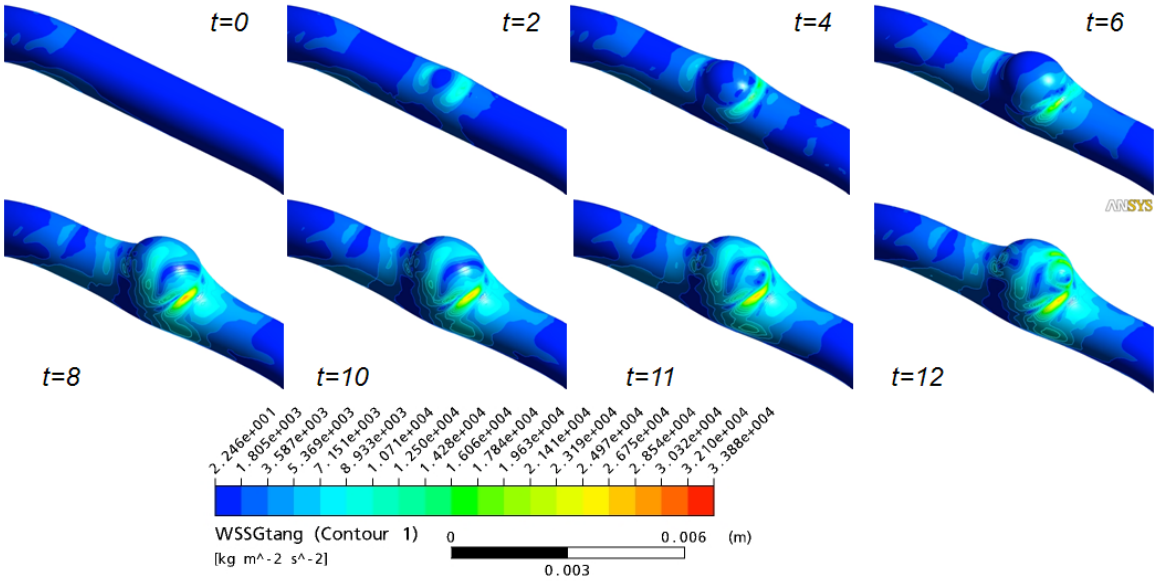
t=0
t=2
t=4
t=6
t=8
t=10
t=11
t=12
ANSYS
2.246e+001
1.805e+003
3.587e+003
5.369e+003
7.151e+003
8.933e+003
1.071e+004
1.250e+004
1.428e+004
1.606e+004
1.784e+004
1.963e+004
2.141e+004
2.319e+004
2.497e+004
2.675e+004
2.854e+004
3.032e+004
3.210e+004
3.388e+004
WSSGtang (Contour 1)
[kg m^-2 s^-2]
0
0.006
(m)
0.003

18

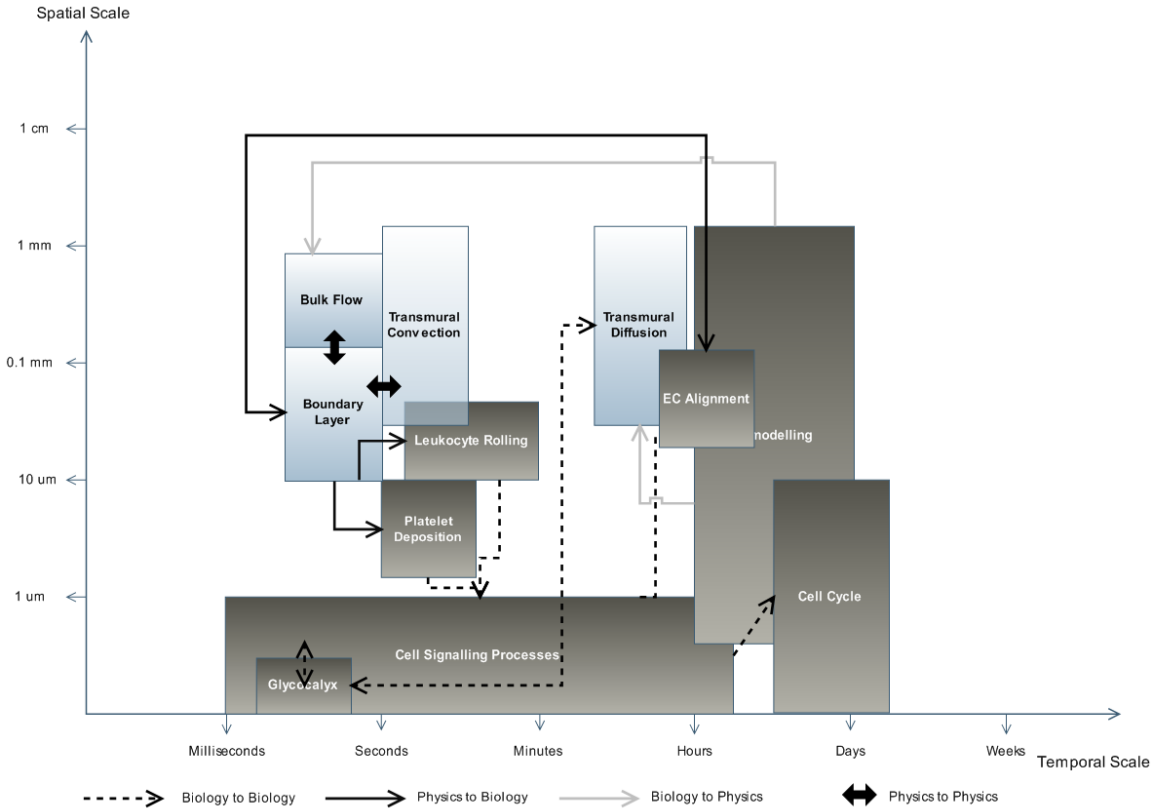
Spatial Scale
1 cm
1 mm
0.1 mm
10 um
1 um
Bulk Flow
Transmural Convection
Boundary Layer
Leukocyte Rolling
Platelet Deposition
Transmural Diffusion
EC Alignment
nodelling
Cell Cycle
Cell Signalling Processes
Glycocalyx
Milliseconds
Seconds
Minutes
Hours
Days
Weeks
Temporal Scale
Biology to Biology
Physics to Biology
Biology to Physics
Physics to Physics

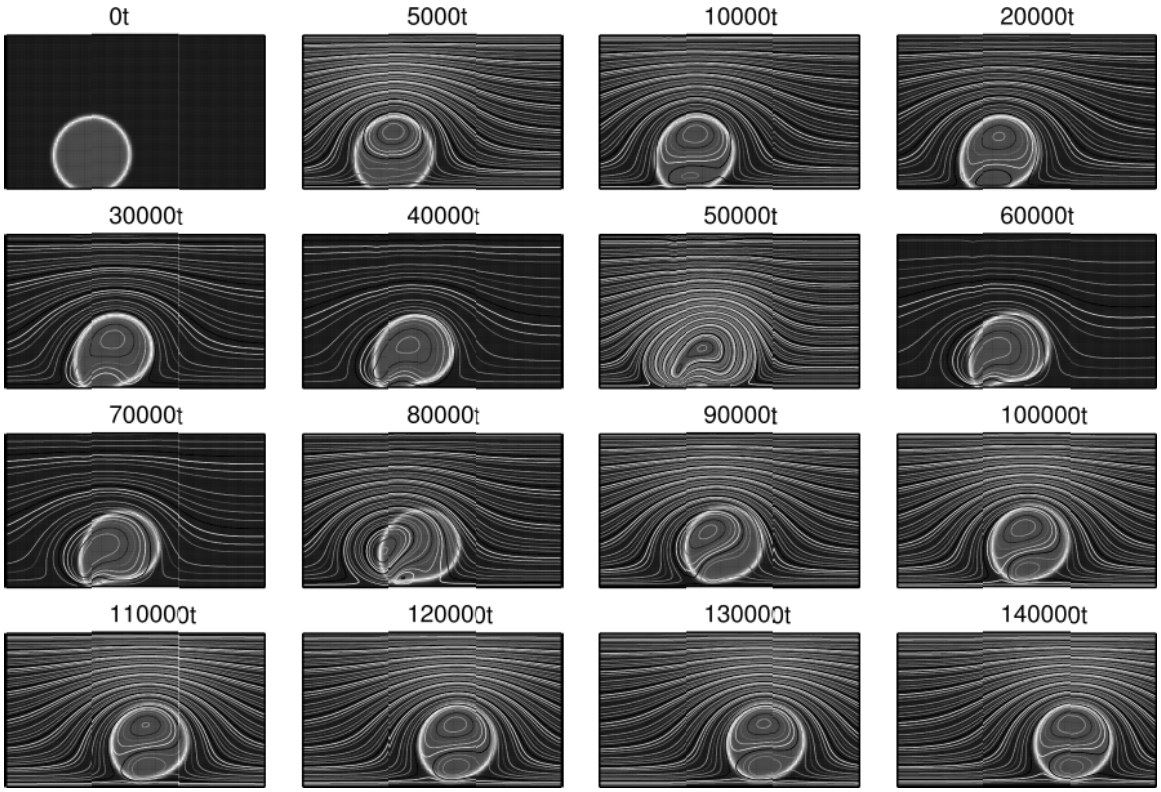
0t
5000t
10000t
20000t
30000t
40000t
50000t
60000t
70000t
80000t
90000t
100000t
110000t
120000t
130000t
140000t

19